JOURNAL OF ZOOLOGICAL SYSTEMATICS AND EVOLUTIONARY RESEARCH

Accepted on 15 September 2015
J Zool Syst Evol Res doi: 10.1111/jzs.12113

[1]*Center for Natural History, Universität Hamburg, Hamburg Germany;* [2]*Naturhistorisches Museum der Burgergemeinde Bern, Bern Switzerland;* [3]*Institute of Biodiversity and Environmental Conservation, Universiti Malaysia Sarawak, Kota Samarahan Sarawak, Malaysia*

The anatomy and structural connectivity of the abdominal sucker in the tadpoles of *Huia cavitympanum*, with comparisons to *Meristogenys jerboa* (Lissamphibia: Anura: Ranidae)

Li Lin Gan[1], Stefan T. Hertwig[2], Indraneil Das[3] and Alexander Haas[1]

Abstract

The tadpoles of many anuran amphibians inhabit lotic habitats and evolved oral devices to adhere to the substratum. Although published anatomical descriptions of rheophilous tadpoles exist, little is known about the modifications in gastromyzophorous tadpoles that possess abdominal suckers and live in torrential sections of streams. We describe the gastromyzophorous tadpoles of *Huia cavitympanum* and *Meristogenys jerboa* from torrential streams of Borneo, with special attention to the anatomy of their abdominal suckers and their relations to cranial structures and musculature. One cranium of *H. cavitympanum* and its associated muscles were computer-reconstructed in three dimensions from serial histological sections. The abdominal sucker and oral sucker comprise a set of muscles and ligaments that attach to internal skeletal structures. Some muscles could be identified to attach directly to soft tissue of the abdominal sucker and most likely contribute to suction. Comparing tadpoles of *H. cavitympanum* to the closely related gastromyzophorous *M. jerboa* reveals differences in external and internal features, such as cornu trabeculae fusion and jaw details. Because of phylogenetic uncertainties, it is unclear whether or not this structural complex evolved once or several times convergently in ranids.

Key words: Anura – Lissamphibia – larval cranium – gastromyzophorous – rheophilous – three-dimensional

Introduction

Altig and Johnston (1989) defined seven ecomorphological guilds of tadpoles that occur only in lotic aquatic environments: the adherent, clasping, fossorial, gastromyzophorous, psammonic, suctorial and semi-terrestrial guilds of tadpoles. Of these, three types of tadpoles are known to live in the current (McDiarmid and Altig 1999): adherent/clasping tadpoles live in slow-flowing sections of streams. They possess ventrals oral discs (for example, *Ansonia leptopus* [Günther, 1872]; personal observation AH). Lotic, suctorial tadpoles possess an enlarged oral disc that forms an oral sucker apparatus (for example, *Ansonia hanitschi* Inger, 1960; *Ascaphus truei* Stejneger, 1899; and some *Litoria* species; Haas and Richards 1998; Haas et al. 2009). Gastromyzophorous tadpoles bear a well-developed abdominal sucker located posterior to the oral sucker that enables these tadpoles to adhere tightly to rocks in strong current or torrential stream sections. Gastromyzophorous larvae have been described in the Ranidae (*Amolop*s; *Huia*; *Meristogenys*; *Rana sauteri* Boulenger, 1909; Annandale and Hora 1922; Hora 1930; Inger 1966; Kuramoto et al. 1984; Yang 1991; Chou and Lin 1997; Malkmus et al. 2002; Matsui et al. 2006; Ngo et al. 2006; Shimada et al. 2007 a,b; Stuart 2008) and the Bufonidae (*Atelopus*, possibly *Sabahphrynus maculatus* (Mocquard, 1890), and some *Rhinella*; Starrett 1967; Duellman and Lynch 1969; Mebs 1980; Lescure 1981; Gray and Cannatella 1985; Lynch 1986; Lindquist and Hetherington 1988; Gascon 1989; McCranie et al. 1989; Cadle and Altig 1991; Inger 1992; Rao and Yang 1994; Lavilla et al. 1997; Matsui et al. 2007; Aguayo et al. 2009; Rueda-Solano et al. 2015). Semiterrestrial tadpoles with expanded abdominal skin (*Thoropa petropolitana* (Wandolleck, 1907); *Cycloramphus valae* Heyer, 1983; Lavilla 1988) are not considered gastromyzophorous herein. Some accounts have been published on the muscles and ligaments that insert to the abdominal suckers in gastromyzophorous larvae (Annandale and Hora 1922; Noble 1929; Kaplan 1997; Aguayo et al. 2009).

The term 'gastromyzophorous' tadpoles was first used by Inger (1966), who described tadpoles from Borneo that inhabit fast flowing, turbulent waters and that have specific morphological characteristics, that is, a well-developed abdominal sucker, expanded oral disc, low caudal fins and massive caudal muscles, correlated to the living in strong current (Altig and Johnston 1989; Altig and McDiarmid 1999; McDiarmid and Altig 1999; Lavilla and de Sá 2001). Large abdominal suckers have been interpreted as an adaptation to high water velocity (Boistel et al. 2005). Although various taxa have conquered high velocity microhabitats successfully with an oral sucker only, among the Bornean fauna, gastromyzophorous larvae of *Huia cavitympanum* (Boulenger, 1893) and *Meristogenys* species have been particularly successful in using very high velocity currents as microhabitat (Inger 1985; Shimada et al. 2007a,b).

The tadpoles of *Huia cavitympanum* are of interest because of their remarkable ability to withstand strong currents and for phylogenetic reasons. The hypothesized phylogeny of *Huia* has undergone several changes and remains controversial (Stuart 2008). Inger (1966) united Asian ranid species with well-developed abdominal suckers into the genus *Amolops*. Subsequently, Yang (1991) recovered three groups within *Amolops*. In his phylogenetic analysis of morphological characters, they were assigned to the genera *Amolops*, *Meristogenys* and *Huia,* respectively. The genus *Meristogenys* was defined by synapomorphy in that analysis: larval upper beak divided and ribbed on its outer surface. Yang (1991) defined the genus *Huia* with one synapomorphy: larvae with scattered glands on the back. Some *Huia* species possess scattered dorsal glands, yet this character is absent in the type species, *H. cavitympanum* (Inger 1985; Stuart 2008). Stuart (2008) and Wiens et al. (2009) suggested *Huia* to be paraphyletic and the type species *H. cavitympanum* to be the sister taxon to the genus *Meristogenys*. They further argued that the remaining species, which Yang (1991) allocated to '*Huia*',

Corresponding author: Alexander Haas (alexander.haas@uni-hamburg.de)
Contributing authors: Li Lin Gan (lgan@dpz.eu), Stefan T. Hertwig (stefan.hertwig@nmbe.ch), Indraneil Das (idas@ibec.unimas.my), Alexander Haas (alexander.haas@uni-hamburg.de)

were in fact basal to *Clinotarsus*. This paraphyly of *Huia* has been corroborated by Pyron and Wiens (2011). Without well-resolved phylogenies, the evolutionary origin of the abdominal sucker in Asian ranid tadpoles remains obscure.

In the present study, we describe the larval cranium and cranial musculature in the gastromyzophorous tadpole of *H. cavitympanum* and compare it to *M. jerboa* (Günther, 1872). In particular, we elucidate the anatomical connectivity of the oral and abdominal suckers and ask how these tadpoles might produce the exceptionally strong suction. We establish primary homology statements that might serve as morphological character states in phylogenetic analyses and thus potentially contribute to the unsolved systematic and taxonomic status of these genera. Specific questions are as follows: (1) What are the structural components of the oral and abdominal suckers in *H. cavitympanum* that enable them to live in torrential streams? (2) Does the larval cranium differ from the closely related species *Meristogenys jerboa*, or are there shared features between *Huia* and *Meristogenys*?

Materials and Methods

Specimens examined

Specimens were collected at Sungei Kipungit, Poring Hot Springs, Gunung Kinabalu Park, Sabah, and Kubah National Park, Sarawak, Malaysia, under permission granted by the State Economic Planning Unit, Sabah Parks, and Sarawak Forest Department, respectively. Tadpoles were found adherent to vertical rock surfaces in foaming cascades. Tadpoles were anesthetized and killed in chlorobutanol (0.2%; Sigma T-5138, Sigma-Aldrich Chemie GmbH Munich, Germany). They were then fixed and stored in pH 7.0-buffered formalin (4%) or (tail parts) in absolute ethanol for DNA analyses. Assignment of tadpoles to *H. cavitympanum* and *M. jerboa*, respectively, was based on published larval descriptions (Inger 1966, 1985; Matsui 1986; Yang 1991; Shimada et al. 2015). Data on the specimens examined are summarized in Table 1. It has been reported before, that suctorial, rheophilous tadpoles deviate from the standard staging table by Gosner (1960; Nodzenski and Inger 1990). With this caution in mind, we still applied Gosner stages to the tadpoles examined (Table 1).

Histology and 3D reconstruction

Two specimens each of *H. cavitympanum* and *M. jerboa* were sectioned serially and (Table 1) analysed in detail. Specimens were decalcified (Dietrich and Fontaine 1975), embedded in paraffin and cut at 10 μm thickness (general protocols in Mulisch and Welsch 2010) on a Microm HE 340E semi-automatic rotary microtome. Sections were stained following a slightly customized Azan protocol (Mulisch and Welsch 2010). Covered slides were then scanned digitally with a Leica DM 6000 B (Leica Mikrosystems, Wetzlar, Germany) microslide scanner microscope. Serial histological sections of specimen ZMH A13122 (*H. cavitympanum*, Gosner Stage 26) were used for three-dimensional reconstruction.

For subsequent reconstruction, episcopic histology image stacks were produced from each of two *M. jerboa* larvae (contrasted episcopic imaging method, modified from Weninger et al. 1998). Photographs were taken from the surface of the lead acetate-impregnated specimen block at intervals of 40 μm, and the cut surface was stained by reaction with sodium sulfide for better contrast (Weninger et al. 1998). Both standard histological sections and image stacks from episcopic microscopy were loaded into AMIRA® software (PC version 32bit; FEI, Hillsboro, Oregon, USA) for three-dimensional reconstruction. Each was segmented with AMIRA® software into muscles (right side), bones (both sides), cartilages (both sides) and selected soft tissues (right side) of the head. Polymesh surfaces were exported from segmented objects, each in separate files. These files were imported into MAYA (Autodesk Inc., San Rafael, California, USA) or MODO® 701 (The Foundry, London, UK; Ablan 2008) 3D visualization software and reduced in polygon count. The export of polymesh surfaces from the data produced artefacts, that is loss of small foramina and slightly inflated objects; these were corrected manually. Sculpting muscle fibre orientations onto the muscles were performed in ZBrush (Pixologic™, Los Angeles, California, USA) software and re-imported including UV and displacement maps into MODO. Coloration, shading, textures and muscle fibre rendering in the 3D models are not meant to replicate actual tissue properties, but rather to facilitate understanding. General muscle fibre orientation for each of the muscles was confirmed by dissection of specimens. We chose object properties so that they resemble cleared and stained (cartilage, bones) or dissected specimens (muscles). Renderings were performed with environmental lighting in MODO and a virtual camera focal length of f = 100 mm.

Whole-mount specimens were cleared and double-stained (Alcian blue; Alizarin red) for examination and drawing of internal skeletal features according to Dingerkus and Uhler (1977), as modified by Taylor and van Dijk (1985). The specimens that were manually microdissected under a Leica stereomicroscope were stained according to the same protocol but not macerated in trypsin, rinsed quickly in 0.5 KOH and then transferred to 30%, 50% and finally 70% ethanol after the Alcian blue staining step.

Photographs of preserved specimens were used for backdrops (Figs 2 and 7) and measurements. They were taken with a calibrated digital microscope (Keyence VHX-500F; Keyence Corp, Osaka, Japan) in dorsal, ventral, and lateral left views. Pictures were edited for tonal balance, sharpness and contrast in Photoshop CS5 (Adobe®, San Jose, California,

Table 1. Material examined.

Species	Catalogue number	Study ID	Gosner stage	Remarks
Huia cavitympanum	ZMH A13123	3-432-Hc	25	Illustration, serial sections
	ZMH A13122	4-432-Hc	26	Serial sections, 3D reconstruction
	ZMH A13139	7-432-Hc	25	Manual dissection
	ZMH A13139	8-432-Hc	26	Cleared and stained
	ZMH A11929	9-211-Hc	28	External characters
	ZMH A11930 (lot)	10-432-Hc	37	External characters
	ZMH A13139	13-432-Hc	26	Manual dissection
	ZMH A11933	15-432-Hc	26	Sem
	ZMH A11926	22-284P-Hc	28	Colour photographs in life
	ZMH A11927 (lot)	23-284-Hc	34	External characters
Meristogenys jerboa	ZMH A13120	1-AJLF032-Mj	25	Serial sections
	ZMH A13121	2-AJLF032-Mj	26	Serial sections
	ZMH A13136	5-AJLF032-Mj	26	Cleared and stained
	ZMH A13136	6-AJLF032-Mj	26	Cleared and stained
	ZMH A13136	11-AJLF032-Mj	25	Manual dissection
	ZMH A13136	12-AJLF032-Mj	26	Manual dissection
	ZMH A11933	14-AJLF032-Mj	26	Sem
	ZMH A13080 (lot)	24-580-Mj	35	Episcopic microscopy, partial 3D reconstruction
	ZMH A13080 (lot)	25-580-Mj	40	Episcopic microscopy, sacrificed
	ZMH A10163	26-507P-Mj	34	Colour photograph in life

USA). Photoshop's 'Photomerge' was used to stitch together partial pictures into more extensive overviews (not shown). Illustrator CS5 (Adobe®) was used for vectorizing drawings, plate assembly and labelling. Colour photographs of selected living tadpoles were taken in the field with a Nikon D100 (Nikon Corp, Tokyo, Japan) and a Sigma Macro 50 mm F2.8 (Sigma Corp, Kanagawa, Japan). Digital photographs of the cleared and stained cranium and hyobranchial apparatus, and plain preserved specimens were used as backdrops for drawings. Contour drawings were made with a graphic tablet (Wacom® Intuos 2CS; Wacom Technology Corp, Vancouver, USA) and Illustrator.

Eye muscles are irrelevant for the scope of this work and were omitted herein. Highly detailed general descriptions of tadpole cranial structures with details on ossifications and foramina have been published elsewhere (Gaupp 1893, 1894; de Beer 1937; de Jongh 1968; Haas 2003; Roček 2003). Foramina and ossifications will be mostly neglected, yet labelled on figures.

High-speed videography

Tadpoles of *M. jerboa* were filmed in the field in a small glass aquarium (200 × 90 × 50 mm). Video sequences (210 or 420 frames per second) were recorded with a Casio Exilim EX FH20 camera.

Homologies and terminology

Criteria of homology assessment applied herein focus on primary homology assessments (de Pinna 1991; Brower and Schawaroch 1996; Richter 2005), such as topological relations and/or connectivity in the context of other structures. We consider muscles to be topographically identical and homologous (i.e. a primary homology; Rieppel and Kearney 2002) if (1) they are similar in form by origin or insertion, by position relative to other muscles and skeletal structures, or by innervation and (2) they pass the conjunction test (i.e. multiple homologues may not exist in the same organism; Patterson 1982). We do not consider secondary homologies formally because we did not perform a phylogenetic analysis. We use anatomical terms for skeletal structures in the tradition of Gaupp (1893, 1894) and de Jongh (1968), preferably in Latinized form, to designate their nature as technical descriptors. We follow muscular terminology that has been discussed for amphibians in previous studies (Haas 1997, 2003; Haas et al. 2006; Kleinteich and Haas 2006, 2011). Terminology for structures of the abdominal sucker was adopted from Kaplan (1997) and Aguayo et al. (2009). Taxonomic names follow Frost (2015).

Results

Figure 1 depicts the two species examined in life. Figure 2 explains features of the external sucker surface. For more details on external features, we refer to published descriptions (Inger 1985; Yang 1991; Shimada et al. 2015).

Cranial of *Huia cavitympanum*

The following description of cranial anatomy is based on *Huia cavitympanum* specimens (Gosner stage 26) ZMH A13122 and ZMH A13139 (specimen 8-432-Hc, and 13-432-Hc).

Neurocranium

The cartilago labialis superior supports the upper keratinized jaw sheath. There is no sign of division between left and right cartilago labialis superior; there is also no sign of subdivision of the cartilago labialis superior into a medial pars corporis and a lateral pars alaris. The cartilago labialis superior is slightly convex (medially), in ventral view. Laterally, it forms an almost triangular plate (Fig. 3A) that presumably represents the pars alaris. It lies parasagittally at an angle of almost 90° to the medial cartilago

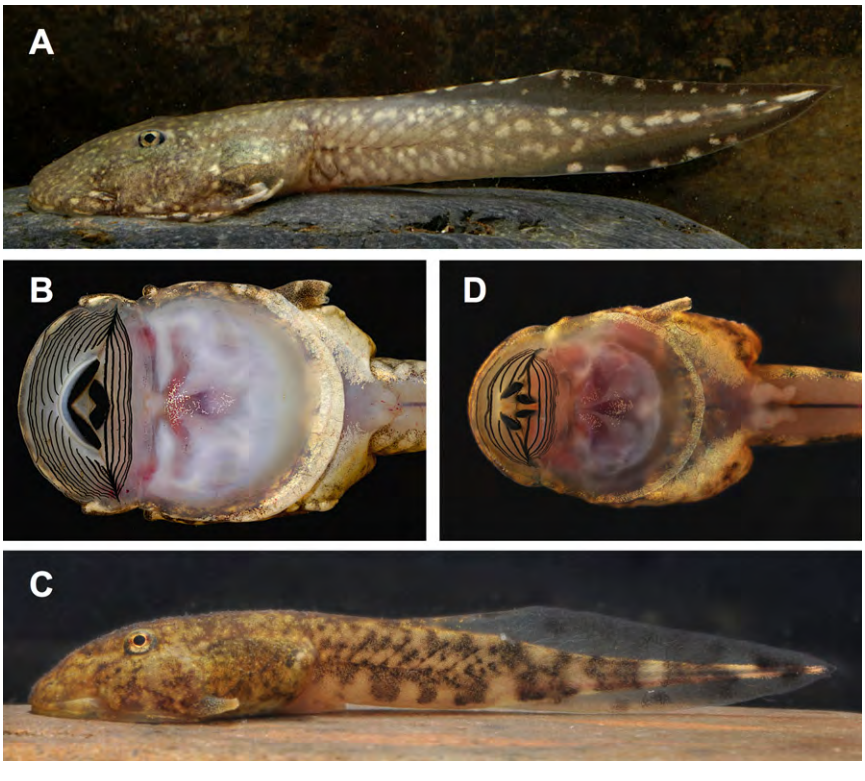

Fig. 1. Tadpoles of *Huia cavitympanum* (ZMH A11926) (A–B) and *Meristogenys jerboa* (ZMH A10163 specimen 26-507-Mj) (C–D) in life. The lateral view shows the strongly dorsoventrally flattened, streamlined body form of *H. cavitympanum* (A, lateral left view); in comparison, the body of *M. jerboa* is less flattened (C, lateral left view). (B) The ventral view of the oral disc and abdominal sucker (same specimen) shows the high number of keratodont rows and undivided jaws sheaths in this species. The comparison of *H. cavitympanum* (B, ventral view) with *M. jerboa* (D, ventral view) reveals the lower number of keratodont row and divided jaws sheaths in *M. jerboa*. Not to scale

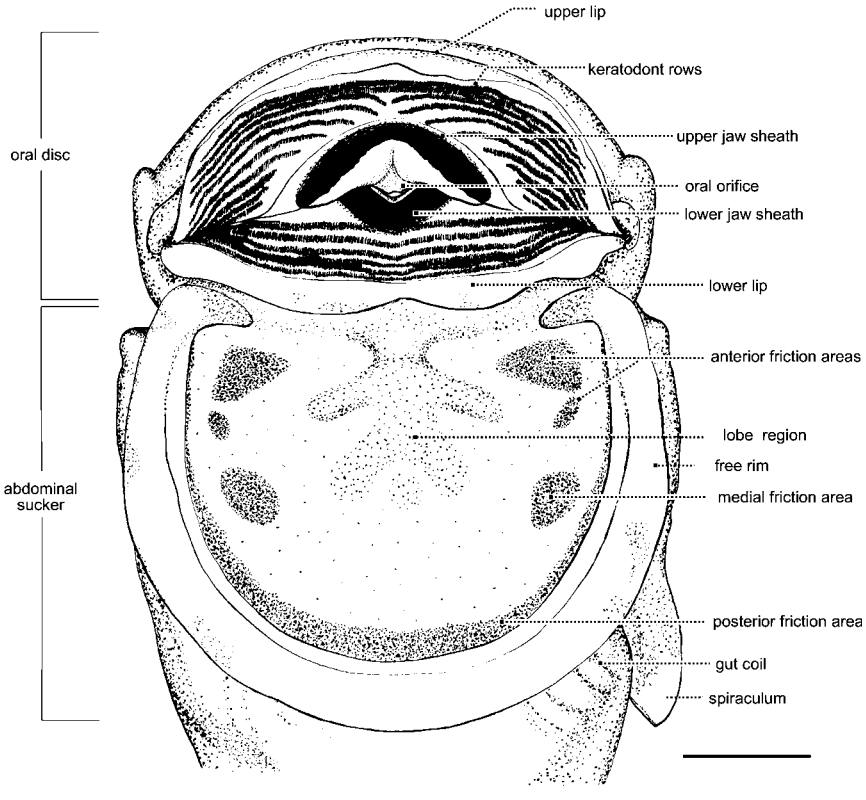

Fig. 2. The drawing of *Huia cavitympanum* tadpole (ZMH A13123) (ventral view, anterior end up) depicts the huge oral disc and abdominal sucker; in particular, the different friction areas as well as the lobe region of the surface of the abdominal sucker are illustrated. The abdominal sucker is limited by its bulging, papillae-free rim. Scale bar: 1 mm

labialis superior part (Fig. 3C). Distally, the cartilago labialis superior forms a processus posterior dorsalis. The cartilago labialis superior articulates dorsally with the cornua trabeculae by joints. Adrostral cartilages are absent.

The cornua trabeculae are two cartilaginous bars that originate from the planum trabeculare anticum (Fig. 3A). As they extend anterolaterally, they descend ventrad, without much curvature in lateral view. The cornua trabeculae are fused for most of their lengths. At 90% of their lengths, they separate at an angle of about 50°. Each is pierced by a small foramen for rostral blood supply. Distally, yet not terminally, each cornu forms a lateral condyle for articulation with the cartilago labialis superior. The relative length of the cornua trabeculae comprises about 33% of total length of the cranium.

The planum trabeculare anticum is a thick cartilaginous plate. It is a confluence between the anterior trabeculae cranii (Fig. 3A) and forms the floor of the anterior cavum cranii. Laterally, the planum trabeculare anticum is confluent with the commissura quadratoorbitalis and lamina orbitonasalis. Septum nasi, tectum nasi, lamina orbitonasalis and processus antorbitalis are the chondrified parts of the capsula nasi at this developmental stage (Fig. 3B). A tectum anterius is developed dorsal to the anterior parts of the brain. At that point, between the lamina orbitonasalis and the taenia ethmoidalis, the foramen orbitonasalis is formed. The trabeculae cranii are two longitudinal rods of cartilage, separated by the basi-cranial space in the mid section of the braincase. At this stage, the fenestra basi-cranialis is occluded with cartilage.

The anterior third of the cartilago orbitalis is chondrified. The cartilago orbitalis is located dorsal to and confluent with the trabeculae cranii. The pila antotica is present. The processus ascendens attaches to the pila antotica (Fig. 3C). The pila antotica forms the anterior margin of the foramen prooticum. The taeniae tecti medialis and transversalis are absent; the taenia tecti marginalis is present. The taenia tecti marginalis connects the cartilago orbitalis to the medial wall of the canalis semicircularis. The pila metoptica separates foramen opticum and foramen oculomotorii. The fenestra frontoparietalis is mostly covered by membrane and partially (laterally) by the frontoparietals (Fig. 3B).

The capsula auditiva dominates the posterior third of the cranium (Fig. 3A, B). The capsula comprises approximately 25% of the cranium length. It is slightly longer than wide, and smoothly rounded, rectangular in shape, caused by the bulging of the semicircular canals inside. The tectum synoticum bridges the two capsulae mediodorsally. The foramen ovale is concealed by the processus oticus in lateral view; an operculum is present. The capsula auditiva is confluent to cartilaginous planum basale (Fig. 3B,C). The planum basale contributes to the ventral margin of the foramen prooticum and articulates with the chorda dorsalis and vertebral column posteriorly. A crest (crista parotica) rises laterally to the canalis semicircularis lateralis. Anteriorly, the processus anterolateralis of the crista parotica fuses to the palatoquadrate as part of the larval processus oticus. The arcus praeoccipitalis is the anterior border of the foramen jugulare. The arcus connects the lateral border of the planum basale to the capsula auditiva.

Viscerocranium

The palatoquadrate is lateral to the neurocranium. The level of the palatoquadrate descends ventrad along its posterior to anterior

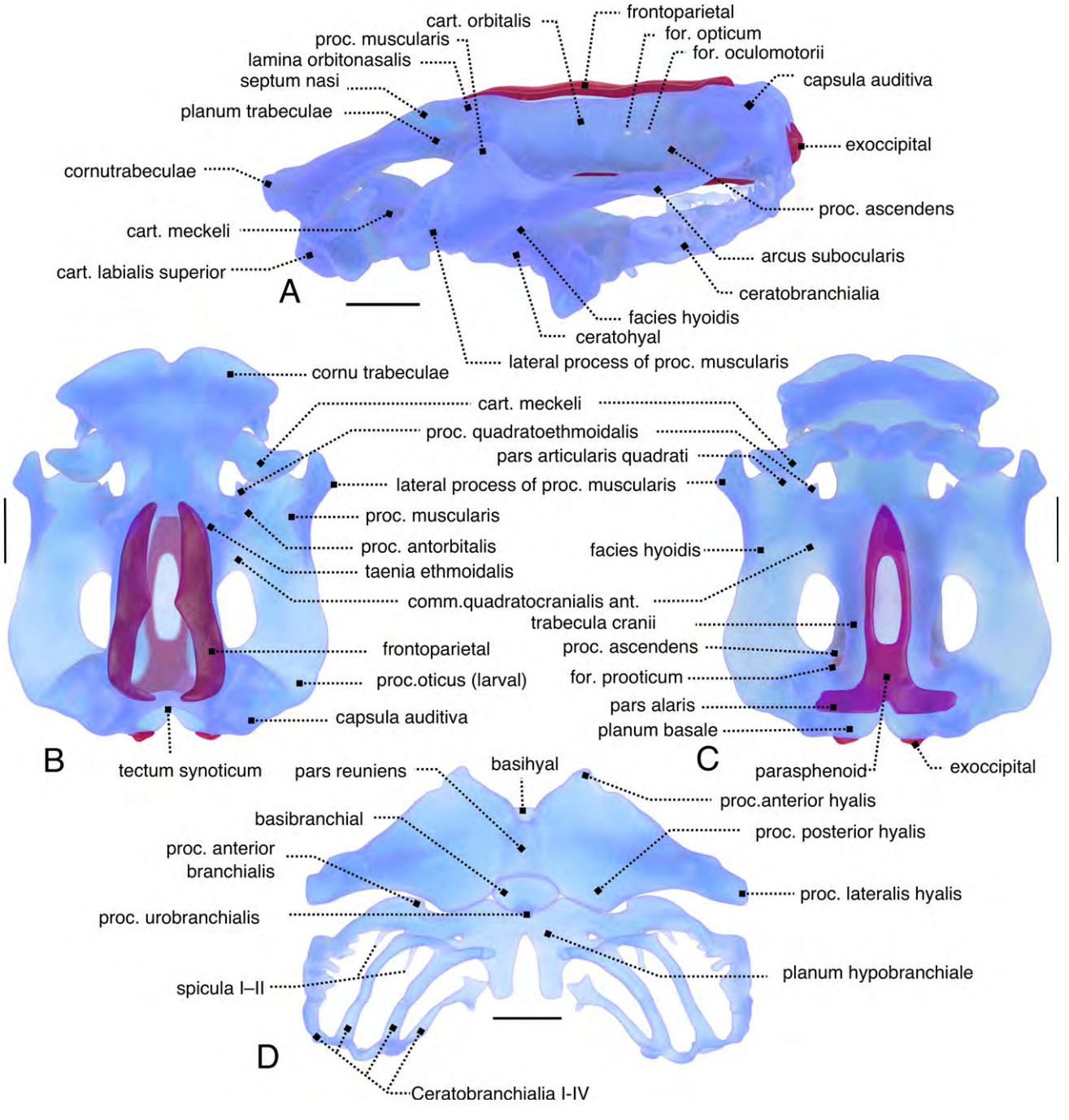

Fig. 3. *Huia cavitympanum* larval cranium. 3D visualization based on a reconstruction of serially sectioned specimen (ZMH A13122), cartilage: blue, bone: purple (A) Lateral view of the cranium, anterior to the left. The cranium of *H. cavitympanum* is strongly chondrified anteriorly and has a long cornu trabeculae. (B) Dorsal view, anterior up, depicts the wide, almost fully fused cornua trabeculae; (C) The ventral view of the cranium, anterior up, shows the position of the jaws. The pars alaris of the parasphenoid extends laterally and supports the capsula auditiva. (D) The ventral view of the isolated hyobranchial apparatus illustrates details of Ceratobranchialia I–IV. The proc. urobranchialis is prominent. Abbreviations: cart., cartilago; comm., commissura; for., foramen; proc., processus. Scale bars: 1 mm

axis. Anteriorly, the pars articularis quadrati articulates with the cartilago meckeli (Fig. 3C). Posteriorly, the palatoquadrate fuses via processus oticus to the processus anterolateralis of the crista parotica. The palatoquadrate is connected anteriorly to the neurocranium by the commissura quadratocranialis anterior and posteriorly by the processus ascendens. The cranium's widest point is at the level of the pars articularis quadrati. A processus pseudopterygoideus is absent. The processus muscularis quadrati originates from the lateral margin of the palatoquadrate, rises dorsad and curves mediad. The processus muscularis projects towards the capsula nasi but does not fuse with it; a commissura quadratoorbitalis (cartilaginous confluence) is absent. Anterolaterally, the processus muscularis forms a prominent lateral process (Fig. 3B). The commissura quadratocranialis anterior bears two processus: the processus antorbitalis and the processus quadratoethmoidalis, both are ligament attachment sites. The articulation with the ceratohyal is located at the ventral surface of the palatoquadrate. The fenestra subocularis (Fig. 3B, C) measures approximately 25% cranial length.

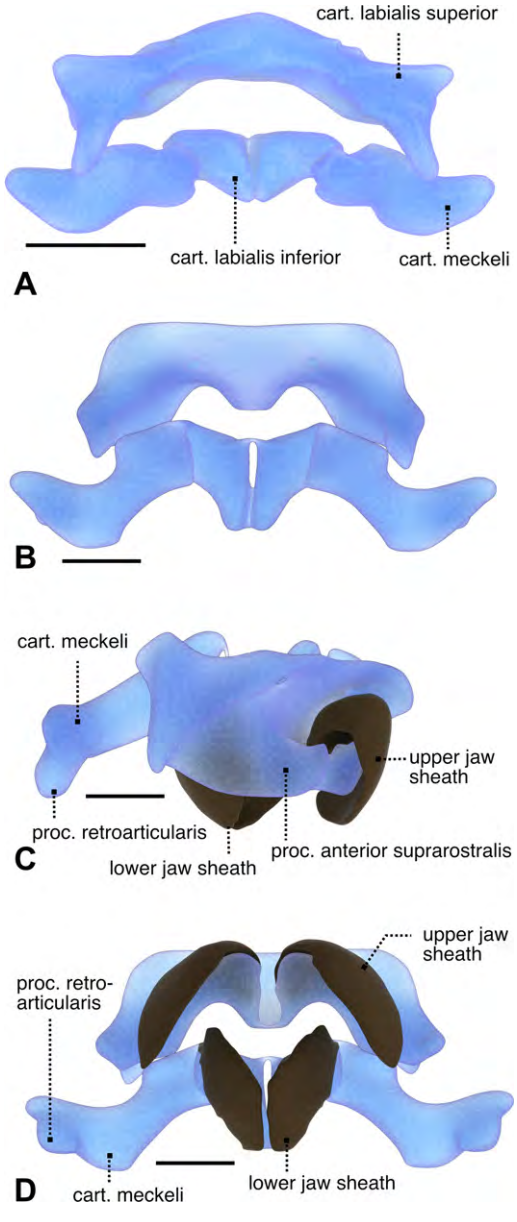

Fig. 4. Upper and lower jaw cartilages in larval *Huia cavitympanum* (A) (ZMH 13122) and *Meristogenys jerboa* (B–D) (ZMH A13080/24-580-Mj). In C, the left jaw sheath is visualized along with the lower jaw beak, whereas in D all beak structures are shown. (A) *H. cavitympanum*, dorsal view. The comparison to *M. jerboa* (B, dorsal view) shows that both species possess robust jaw cartilages. Arrangement of the cart. meckeli is more transverse in *H. cavitympanum* and the cart. labialis inferior is relatively more extensive in the anteroposterior axis in *M. jerboa*. The oblique lateral view, anterior pointing right, (C) reveals that in *M. jerboa* the cartilago labialis superior is distinctly different from that of *H. cavitympanum* by possessing a ventral processus directed anteriorly, to which refer as proc. anterior suprarostralis, and a dorsal edge protruding anteriorly above it. The keratinized upper jaw sheath curls into the cavity between the dorsal edge and the ventral processus for fastening. Abbreviations: cart., cartilago; proc., processus. Scale bars: 1 mm

The cartilago meckeli is S-curved (Fig. 4A). Medially, it articulates with the cartilago labialis inferior. Usually, a thin intramandibular cartilaginous confluence (commissura intramandibularis) connects cartilago labialis to cartilago meckeli in tadpoles. This commissura intramandibularis is absent in *H. cavitympanum*; the coupling between the two cartilages is established by ligaments alone. In anterior view, the cartilagines infrarostrales are V-formed at an angle of approximately 75° (Fig. 4A). The cartilagines infrarostrales are flexibly connected medially by a cartilaginous and fibrous symphysis; they bear the horny sheath of the lower jaw.

The ceratohyal's medial part is a horizontal plate. The processus anterior hyalis projects from the anterior margin and the processus posterior hyalis from the posterior margin of the ceratohyal; the processus anterolateralis hyalis is not formed as a distinct process. The ceratohyal extends beyond the condylus articularis and forms the processus lateralis hyalis, which bears the crista lateralis hyalis, that demarcates the insertion of the musculus orbitohyoideus. The pars reuniens connects the ceratohyalia medially. It is a flexible synchondral joint. Posteriorly, the pars reuniens connects to the basibranchiale (Fig. 3D). The unpaired basibranchiale is confluent with the plana hypobranchialia posteriorly; the connection is established by synchondroses. The ventral surface of the basibranchiale forms a well-developed and medially located processus urobranchialis that points posteriorly and ventrally. The basihyal is an isolated, subspherical cartilage anterior to the pars reuniens and embedded in the transversely oriented ligamentum interhyale.

The planum hypobranchiale is thickened anteriorly and is laterally confluent with the Ceratobranchial I. For one-third of their lengths, the plana hypobranchialia are interconnected synchondrotically. Posterior to the connection to Ceratobranchial I, the planum hypobranchiale is confluent to Ceratobranchial II by a cartilaginous confluence. Ceratobranchial III originates on the ventral surface of the planum hypobranchiale. A processus anterior branchialis projects anteriorly from the Ceratobranchial I (Fig. 3D). Proximally, Ceratobranchial I and II each bear a spiculum. They have a length of approximately 25% of the respective ceratobranchial. Proximally, Ceratobranchial II and III are bridged confluently by the processus branchialis. Ceratobranchial IV is not connected to the planum hypobranchiale. At its proximal end, the Ceratobranchial IV forms an anterior and posterior projection. Distally, all ceratobranchialia are confluent by commissurae terminales and curve dorsad.

Osteocranium

The exoccipitals are present in the Stage 26 specimens examined (Fig. 3A–C). They are medially detectable on the arcus occipitalis' surface in cleared and stained specimens. At this stage, the exoccipital covers the arch for approximately two-thirds (ZMH A13139 specimen 8-432-Hc) or all of its length (ZMH A13122). The frontoparietals are long and narrow ossifications (Fig. 3B) at the dorsal border of the cartilago orbitalis. Anteriorly, the frontoparietals end at the level of the foramen orbitonasalis. Posteriorly, the frontoparietals extend onto the tectum synoticum. The parasphenoid covers the ventral aspect of the braincase between the trabeculae cranii and the capsulae auditivae (Fig. 3C). It is T-shaped: the medial anterior pars cultriformis and the posterolateral partes alares. The pars cultriformis assumes the form of a long and oval ring, and covers only parts of the basis cranii. Anteriorly, it begins approximately at the level of the anterior edge of the commissura quadratocranialis anterior. Posteriorly, the pars alaris of the parasphenoid extends laterally and supports the floor of the capsula auditiva.

Cranial musculature and abdominal sucker musculature in *Huia cavitympanum*

Eight muscles belong to the nervus trigeminus innervated group: musculus levator mandibulae internus, m. lev. mand. externus

superficialis, m. lev. mand. externus profundus, m. lev. mand. articularis, m. lev. mand. longus superficialis, m. lev. mand. longus profundus, intermandibularis, and m. mandibulolabialis inferior. M. lev. mand. lateralis and m. submentalis were not detected in the specimens and stages examined. Origins and insertions are summarized in Table 2 and Fig. 5.

The m. lev. mand. externus superficialis and are very thin, comprising only few fibres. The m. lev. mand. externus superficialis runs dorsal to the m. lev. mand. externus profundus and m. lev. mand. lateralis. The m. lev. mand. articularis crosses the m. lev. mand. internus dorsally. The m. lev. mand. internus arises from the anteroventral part of the capsula auditiva and the planum basale. It extends anteriorly and traverses the pars articularis quadrati ventral to all other muscles of the levator series. It inserts on the most lateral prominence of cartilago meckeli. The m. lev. mand. longus superficialis has two heads (Fig. 5B). The two origins are as follows: posteriolateral border of the arcus subocularis and processus ascendens of the palatoquadrate. The m. lev. mand. longus profundus is the largest muscle of the masicatory muscles. It runs dorsal to the cartilago meckeli where it continues anteriorly with a long tendon that inserts at the lateral part of the cartilago labialis superior.

The two most anterior mandibular muscles (m. intermandibularis, m. mandibulolabialis inferior) originate from the anterior face of the cartilago meckeli. The m. mandibulolabialis inferior has two origins: processus ventromedialis and anterior face concavity of the cartilago meckeli.

The nervus facialis innervated muscles comprise seven muscles in *Huia cavitympanum*: m. orbitohyoideus, m. suspensoriohyoideus, m. suspensorioangularis, m. quadratoangularis, m. hyoangularis, m. interhyoideus (pars cutanea) and m. interhyoideus (proper). The m. orbitohyoideus and m. suspensoriohyoideus act exclusively on the ceratohyal. The m. suspensoriohyoideus is deep to the m. orbitohyoideus, partly covered by it, and has a very broad origin, visible in lateral view (Fig. 5A).

The m. suspensorioangularis reaches far posteriorly. The m. hyoangularis is relatively thick in cross-sectional area. The m. interhyoideus is divided into two parts; the m. interhyoideus pars cutanea is unique and inserts into the abdominal sucker, whereas the m. interhyoideus (proper) interconnects the ceratohyalia. We consider the former a separation from the latter based on proximity, origin and fibre arrangement.

The branchial muscles comprise m. constrictor branchialis II, m. constrictor branchialis III, m. constrictor branchialis IV, m. lev. arcuum branchialium I, m. lev. arcuum branchialium II, m. lev. arcuum branchialium III, m. lev. arcuum branchialium IV, m. subarcualis rectus I (dorsal and ventral heads), m. subarcualis rectus II–IV, m. subarcualis obliquus, m. tympanopharyngeus, the m. diaphragmatopraecordialis and m. diaphragmatobranchialis. The m. subarcualis obliquus originates at the processus branchialis III and the ceratobranchial III and inserts onto the processus urobranchialis of the basibranchial. The strongly developed m. diaphragmatopraecordialis takes origin from the diaphragm and close to the planum basale and inserts broadly to the medial part of the abdominal sucker. The muscle's identity is not obvious, yet we argue that it has the same position and connectivity as in other tadpoles and, more specifically, shares innervation patterns (Cranial Nerve VII) with the m. diaphragmatopraecordialis of other tadpoles. The muscles consist of various tracts of bundles that we reconstructed as three major units, however, subsumed under the same name. The m. rectus cervicis inserts on the proximal part of the ceratobranchial III. The m. rectus abdominis runs from the diaphragm to the posterior part of the abdominal sucker. The laryngeal muscles (m. dilatator laryngis, m. constrictor laryngis) are present.

In sum, the abdominal sucker obtains muscular connectivity by six muscles (Fig. 6A, B; Table 2): musculus mandibulolabialis inferior, m. intermandibularis, m. interhyoideus pars cutanea, m. diaphragmatopraecordialis, m. rectus cervicis and m. rectus abdominis. In addition, we identify and name seven ligaments that fasten the tissue of the abdominal sucker: ligamentum submaxillare internum, lig. submaxillare laterale, lig. submaxillare transversale, lig. subquadratum, lig. subhyoideum longum, lig. subhyoideum inferius and lig. subhyoideum mediale. As further soft tissue structures, the diaphragm, that is the branchial chamber wall, and the pericardium are attached dorsally to the posterior half of the abdominal sucker connective tissue.

The lobe region (Fig. 2) of the abdominal sucker is connected to four of the mentioned structures: m. intermandibularis, lig. submaxillare internum, lig. submaxillare laterale and lig. submaxillare transversale. The anterior friction area is fastened medially by the lig. subhyoideum mediale. The posterior friction area is supported by the lateral parts of the diaphragm, the branchial chamber wall and the m. rectus abdominis. The intermediate central lobe region is connected to the m. interhyoideus pars cutanea, lig. subquadratum, lig. subhyoideum longum and the very short lig. subhyoideum inferius, the medial parts of the diaphragm, the branchial chamber wall, and m. rectus abdominis, the pericardium, m. diaphragmatopraecordialis and m. rectus cervicis.

Comparison to *Meristogenys jerboa*

The following notes are based on *M. jerboa* specimens (Gosner stage 26) ZMH A13136 (specimen 5-AJLF032-Mj, and 6-AJLF032-Mj). The neurocranium in *M. jerboa* is similar to that in *H. cavitympanum* (Fig. 3B and 7A). However, anterolaterally, the processus muscularis does not form a lateral process, and the cornua trabelulae are fused for only half of their lengths (Fig. 7A). The viscerocranium in *M. jerboa* specimens differs from that of *H. cavitympanum* notably in the processus branchialis III points anteriorly but does not connect Ceratobranchial II to Ceratobranchial III, and Ceratobranchial III fuses with the Ceratobranchial II on the lateral part of the planum hypobranchiale (Fig. 7B, Table 3). The muscles and ligaments examined and their general arrangement in relation to the abdominal sucker where identical in the two species.

Discussion

Suctorial tadpoles of various frog lineages have conquered torrential habitats independently (Gradwell 1973; Altig and Johnston 1989; McCranie et al. 1989; Haas and Richards 1998; McDiarmid and Altig 1999; Coloma 2002; Matsui et al. 2005; Pramuk and Lehr 2005; Shimada et al. 2011; Randrianiaina et al. 2012; Zachariah et al. 2012). These suctorial tadpoles have evolved certain morphological features convergently. The convergent evolution indicates that these features are directly related to physical requirements for a life in swift waters. Most suctorial tadpoles feature: oral disc enlarged and thick-rimmed (oral sucker); often increased number of keratodont rows; tail fins reduced to the posterior half of the tail; depressed body; extended snout; strong beaks; dorsal position of the eyes; relatively large nares; relatively large body size; and strong tail muscle and thick skin.

Many suctorial species rely exclusively on sucker-like oral discs in order to adhere to rocks and hold position in swift water. The presence of an abdominal sucker posterior to the oral disc is

Table 2. List of cranial muscles and their origin and insertion sites in *Huia cavitympanum*.

Musculus	Origin	Insertion	Comment
Mandibular group			
Levator mandibulae longus superficialis	Posterolateral part and dorsal face of palatoquadrate and proc. Ascendens (medial head)	Proc. Dorsomedialis of cartilago meckeli	
Levator mandibulae longus profundus	Posterior part and dorsal face of palatoquadrate (arcus subocularis)	Lateral face of cartilago labialis superior	
Levator mandibulae externus profundus	Anterior part and medial side of proc. Muscularis quadrati	Lateral face of cartilago labialis superior	
Levator mandibulae externus superficialis	Anteromedial base of proc. Muscularis quadrati	Lateral face of cartilago labialis superior	Incompletely separated from levator mandibulae externus profundus
Levator mandibulae articularis	Medially from base of proc. Muscularis quadrati	Dorsolaterally at cartilago meckeli	
Intermandibularis	Anterior part of cartilago meckeli	Median raphe	Some muscle fibres insert at the abdominal sucker
Mandibulolabialis inferior	Anterior part of cartilago meckeli, proc. Ventromedialis, medial face of cartilago meckeli at base of proc. Dorsomedialis	Lower lip, oral sucker	
Levator mandibulae internus	Ventral side and anterior part of planum basale	Lateral part of cartilago meckeli	
Hyoid group			
Hyoangularis	Lateral part of ceratohyale	Broadly at proc. Retroarticularis of cartilago meckeli	
Quadratoangularis	Anterior on ventral surface of palatoquadrate	Proc. Retroarticularis of cartilago meckeli	
Suspensorioangularis	Posterior on ventral surface of palatoquadrate, reaching level of larval processus oticus	Proc. Retroarticularis of cartilago meckeli	
Orbitohyoideus	Dorsal and anterior margin of proc. Muscularis quadrati and partially from lateral surface of that process	Proc. Lateralis of ceratohyale	
Suspensoriohyoideus	Lateral surface of proc. Muscularis quadrati and neighbouring arcus subocularis	Proc. Lateralis of ceratohyale	Medial to orbitohyoideus and mostly covered by the latter in lateral view
Interhyoideus (pars cutanea)	Proc. Lateralis of ceratohyale	Medial part of the abdominal sucker	
Interhyoideus (proper)	Proc. Lateralis of ceratohyale	Median raphe	
Diaphragmatopraecordialis	Dorsal part of 'diaphragm', close to planum basale	Broadly on medial part of abdominal sucker	Although far posterior, innervation by Cranial Nerve VII confirmed its assignment to the hyoid group
Branchial group			
Levator arcuum branchialium I	Lateral edge of palatoquadrate (arcus subocularis) and proc. Oticus	Dorsolateral parts of Ceratobranchiale I	
Levator arcuum branchialium II	Posterior surface of palatoquadrate at proc. Oticus	Commissura terminalis I and lateral parts of Ceratobranchial I	
Levator arcuum branchialium III	Capsula auditiva, posterior and dorsal to larval proc. Oticus	Commissura terminalis II	
Levator arcuum branchialium IV	Capsula auditiva, posterior to proc. Oticus	Commissura terminalis III	
Tympanopharyngeus	Ventral face in posterior part of capsula auditiva	Posterior section of Ceratobranchiale IV	
Constrictor branchialis II	Commissura terminalis I	Medial part of Ceratobranchiale II	
Constrictor branchialis III	Commissura terminalis II	Proc. Branchialis III	
Constrictor branchialis IV	Commissura terminalis II	Medial part of Ceratobranchiale III	
Subarcualis rectus I (dorsal head)	Posterior face at medial part of ceratohyale	Medial part of Ceratobranchiale I	
Subarcualis rectus I (ventral head)	Posterior face at medial part of ceratohyale	Proc. Branchialis III	
Subarcualis rectus II–IV	Medial part of Ceratobranchiale II	Medial part of Ceratobranchiale IV	
Subarcualis obliquus	Medial part of Ceratobranchiale III	Proc. Urobranchialis	
Diaphragmatobranchialis	'Diaphragm'	Commissura terminalis III	
Spinal group			
Geniohyoideus	Planum hypobranchialis and proximal origin of ceratobranchiale iii	Cartilago labialis inferior	
Rectus abdominis	'Diaphragm', in extension of posterior rectus abdominis	Posterior part of the abdominal sucker	
Rectus cervicis	'Diaphragm' and ventral body wall (abdominal sucker)	Medial part of ceratobranchiale III	

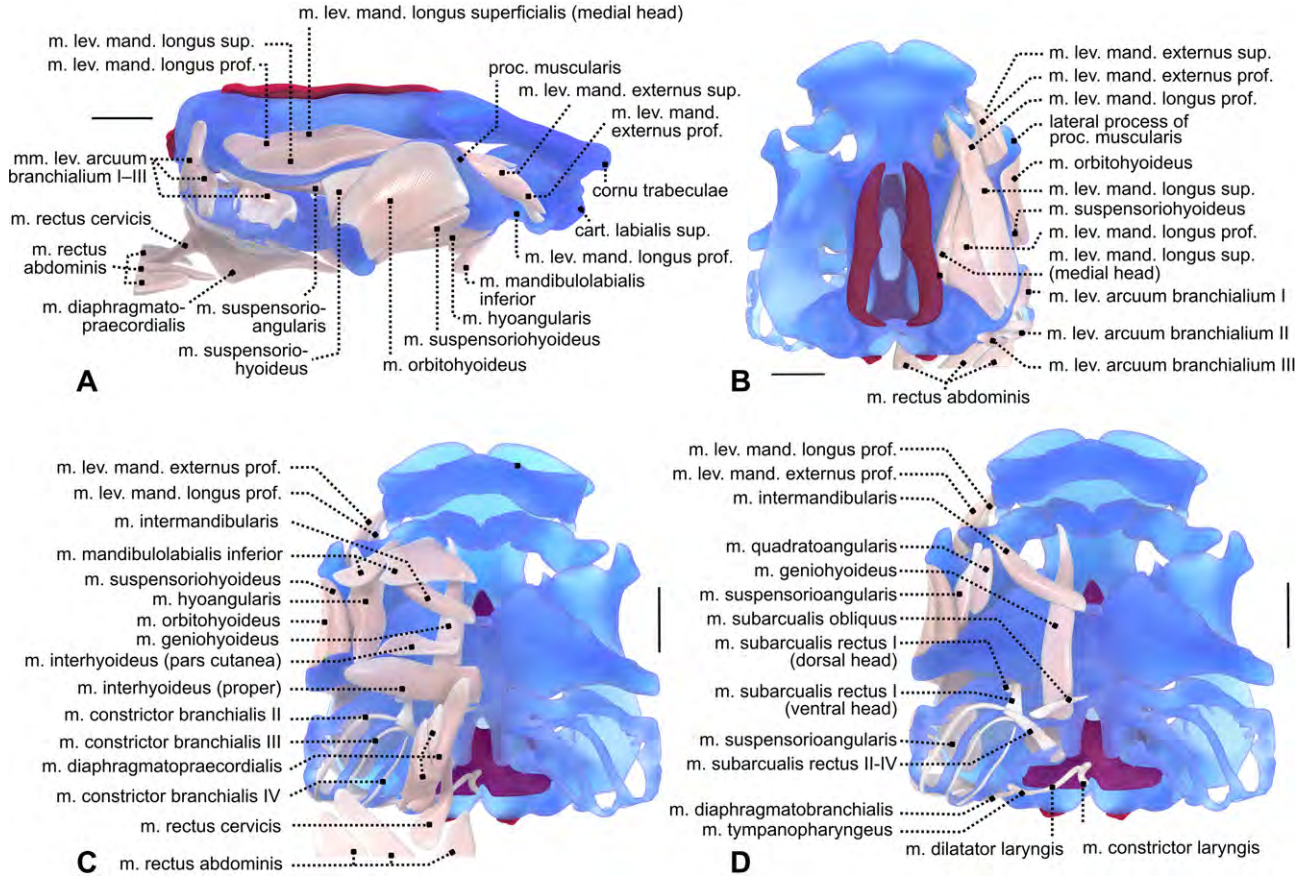

Fig. 5. Cranial skeleton and cranial muscle topology of *Huia cavitympanum.* 3D visualization based on a reconstruction of serially sectioned specimen (ZMH A13122), cartilage: blue, bone: purple, muscle (reconstructed on right side only): light brown. (A) lateral view, anterior to the right; (B) dorsal view, anterior up; (C) ventral view; (D) ventral view, in which several of the superficial muscles have been removed to expose deeper musculature. Abbreviations: cart., cartilago; lev., levator; mand., mandibulae; m., musculus; mm., musculi, prof., profundus; sup., superficialis. Scale bars: 1 mm

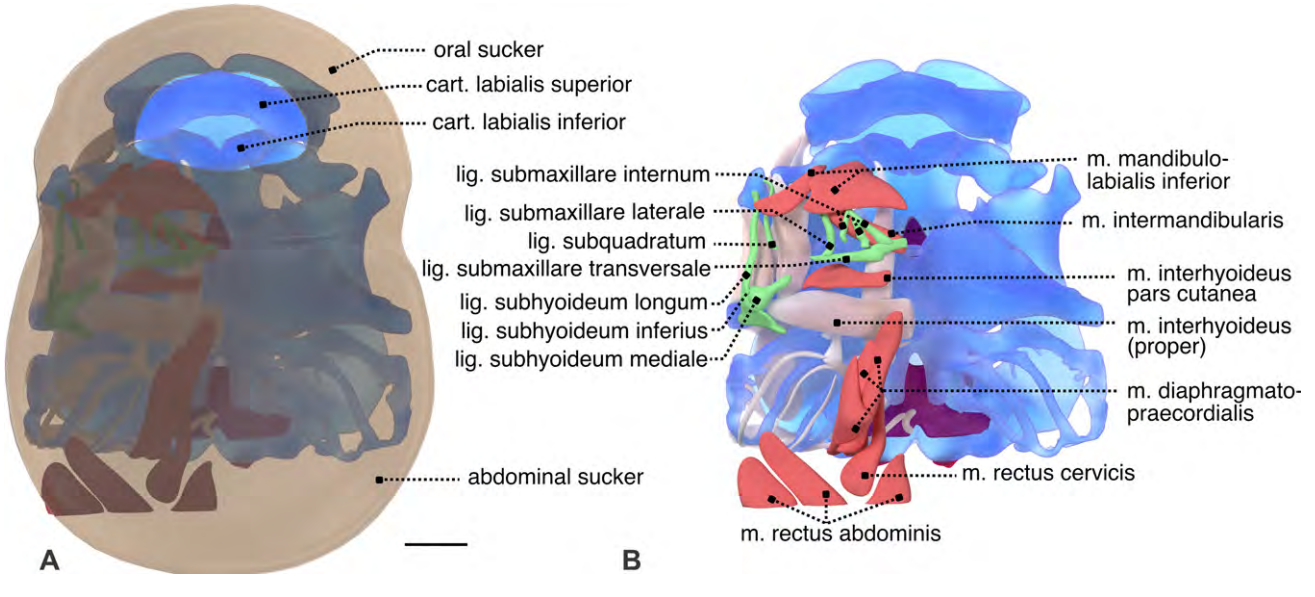

Fig. 6. Cranial skeleton and cranial musculature of *Huia cavitympanum* (ventral view, anterior side up) depicted with (**A**) and without abdominal suckers surface (**B**). 3D visualization based on a reconstruction of serially sectioned specimen (ZMH A13122) shows the musculature and the ligaments that are connecting to the oral- and abdominal suckers' surfaces; cartilage: blue; bone: purple; muscles with connection to the sucker apparatus: red; ligaments connected to the oral disc or abdominal sucker: green. Abbreviations: cart., cartilago; lev., levator; lig., ligamentum; mand., mandibulae; m., musculus. Scale bar: 1 mm

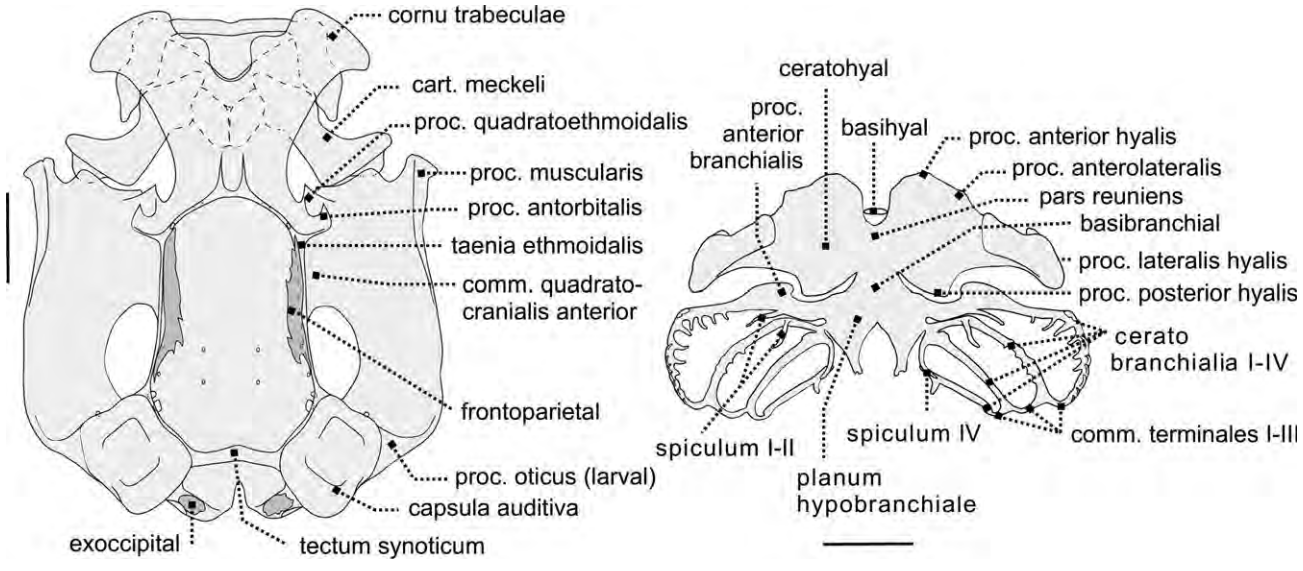

Fig. 7. Neurocranium, dermatocranium and jaws (A, dorsal view, anterior side up) and hyobranchial apparatus (B, dorsal view) of larval *Meristogenys jerboa*. (A) Drawing of a cleared and stained specimen (ZMH A13136 specimen 6-AJFL032-Mj) reveals divided cornu trabeculae. (B) The Ceratobranchial III connects to the lateral part of the planum hypobranchiale. Abbreviations: cart., cartilago; comm., commissura; proc., processus. Cartilage: light grey; bone: dark grey. Scale bars: 1 mm

more rare in the Anura (see above). The presence of a large abdominal sucker is the most striking feature in tadpoles of *Huia* and *Meristogenys*. Because the above mentioned features of suctorial tadpoles apply to them too, we consider these gastromyzophorous tadpoles a subclass of suctorial tadpoles in general.

It was shown in bufonid species, that the abdominal sucker provides suction force in addition to that of the oral disc and buccal pump (Aguayo et al. 2009). It is positioned posterior to the mouth, easily sealed off and does not interfere with feeding or ventilation water flow through the mouth contrary to species that rely exclusively on oral sucker structures (e.g. *Ascaphus*, Gradwell 1973; *Ansonia*, Haas et al. 2009). The power of such abdominal suckers was demonstrated by Hora (1923), who performed lifting experiments and reported that tadpoles could lift an object out of water that was about 60 times the tadpoles' mass. We observed in the field that large *Huia* tadpoles were difficult to manually lift off the rock without causing harm to the animal. Forces of the sucker mechanism include friction (Fig. 2, friction areas) and suction (Kaplan 1997). The amounts of each of the contributing physical forces remain to be shown.

In the present study, we identify the muscular and major ligamentous structures that connect to the soft tissue of the abdominal sucker and likely influence the functioning of that structure, either actively (muscle) or as transduction chain (ligament connected to moving skeletal element). We are well aware that functional reasoning based on structural connectivity faces limitations. *In vivo* testing has not been performed because the larvae of *H. cavitympanum* and *M. jerboa* have proven sensitive to being removed from their microhabitat and quickly died in captivity.

The abdominal sucker possesses a flat central roof and a raised bulging rim, reminiscent of a common suction bell. Our study identifies structures that attach to the abdominal sucker's internal roof surface (ligaments and muscles; Fig. 6). By anatomical conjecture, we infer that centrally attached ligaments and muscles lift up the centre of the abdominal sucker to create negative pressure, while the thick soft rim serves as sealing to the substrate. A muscle thick in cross section that could contribute to this hypothesized suction force is the m. diaphragmatopraecordialis, which is thick in cross section (Fig. 6). The anterior part of the abdominal sucker is under the action of the m. interhyoideus pars cutanea and the m. intermandibularis. Ligaments that attach to the abdominal sucker likely support the suction force (Fig. 6) by

Table 3. Summary of larval *Huia cavitympanum* and *Meristogenys jerboa* comparison.

Compared characters	*Huia cavitympanum*	*Meristogenys jerboa*
External features		
Body shape	Dorsoventrally flattened	Less flattened than *Huia cavitympanum*
Oral disc	LTRF: III: 8–8 (9–9)/ 1–1: V (Yang 1991; present study)	LTRF: 7 (4–7)/9 (1 + 9) (present study)
Maximum eye diameter	1.41 mm (n = 10)	1.48 mm (n = 10)
Tail fin	Dark pigmented border	No dark pigmented border
Maximum total body length	56.39 mm	37.61 mm
Keratinized spinules	Absent	Present
Internal features		
Lateral process of processus muscularis	Lateral process of processus muscularis strongly developed	Absent
Cornu trabeculae	Cornua trabeculae fused for 90% of length	Cornua trabeculae fused for 50% of length
Cartilago labialis superior	U-shaped in ventral view	Complex shape with processus anterior suprarostralis (anchoring of the beak) and dorsal extension
Processus branchialis	Confluence between Ceratobranchial II and Ceratobranchial III	Processus points anteriorly from Ceratobranchial III but does not fuse with Ceratobranchial II
Ceratobranchial III	Connects to the ventromedial part of the planum hypobranchiale	Connects to the lateral part of the planum hypobranchiale

LTRF, labial tooth row formula.

transmitting forces from the jaw's and ceratohyal's movements to the sucker. Ligaments of the abdominal sucker have been described in *Amolops ricketti* and *Rhinella quechua* (Noble 1929; Aguayo et al. 2009; respectively). Both studies described the same five ligaments that attach to the soft tissue of the abdominal sucker (the paired subhyoideus ligaments, the paired subquadrate ligaments and the submaxillary ligament). The subquadrate ligaments and the subhyoideus ligaments fan out as they approach the abdominal sucker. The submaxillary ligament maintains a narrow base. In *H. cavitympanum*, we distinguish a total of seven paired ligaments attaching to the abdominal sucker (Fig. 6c). In *H. cavitympanum*, the ligaments do not fan out, only the lig. submaxillare internum forms three strands towards the inner wall of the abdominal sucker. In *Atelopus ebenoides* Rivero, 1963 tadpoles, Kaplan (1997) described only one ligament that attached to the abdominal sucker. This ligament in *A. ebenoides* occupies nearly the same position as the ligament lig. submaxillare laterale in *H. cavitympanum* and *M. jerboa*. It has been speculated that in *Amolops*, the attached ligaments would help to lift the disc as the body arches through the contraction of some of the muscles (Annandale and Hora 1922; Noble 1929; Hora 1930); however, this remains unconfirmed. It seems more likely, that the posterior part of the abdominal sucker could be lifted up by the m. rectus cervicis.

The muscular connectivity of the abdominal sucker in *H. cavitympanum* tadpoles resemble that described for *Amolops ricketti* (Boulenger, 1899; Noble 1929: as *Staurois*) and *Atelopus* larvae (Kaplan 1997) and includes several muscles that, in generalized tadpoles, are related to feeding and the gill irrigation mechanism (Gradwell 1972b). Noble (1929) attributed the work for active suction in *Amolops* tadpoles to three muscles: the m. rectus abdominis, m. diaphragmatopraecordialis medialis and m. subbranchialis (Noble's terms). For *Huia* and *Meristogenys*, we attribute the active suction mechanism to the six muscles that attach to the abdominal sucker (Table 2, Fig. 6). Muscles involved in the suction mechanism of the abdominal sucker are more strongly developed (m. diaphragmatopraecordialis) than their homologues in non-suctorial ranids tadpoles (Haas 2003: fig. 10b) or have evolved specialized slips to the sucker's connective tissue (intermandibularis, m. interhyoideus pars cutanea).

In our high-speed video recordings of *M. jerboa* (Video S1), we perceived that disengagement from glass surface was initiated by outward rotation (wide opening) of the lower jaw that may relax the anterior sealing of the abdominal sucker. Jaw movements also played a role in locomotion (Video S1): first, the tadpole opened its mouth very wide (outward rotation of both cartilago labialis superior and lower jaw), then engaged onto the substrate with the upper lip and upper jaw anteriorly, and subsequently pulled the lower jaw and the body anteriorly. The jaw levators that connect to either the suprarostral or infrarostral cartilages are strongly developed in these tadpoles and might play a prominent role in pulling the tadpole forward during substrate-bound locomotion and feeding. Furthermore, the m. suspensorioangularis (Fig. 5) is very long in the species examined. Long fibres can translate into a wide range of motion of the lower jaw (Larson and Reilly 2003; Vera Candioti et al. 2004; Vera Candioti 2005) likely necessary for disengagement of the abdominal sucker. In our video recordings, successive cycles of jaw movements were accompanied by synchronous cyclic activity in the anterior dome region (attachment area of m. interhyoideus pars cutanea and m. diaphragmatopraecordialis). During surface crawling, tadpoles remained attached to the glass at all times. This has also been observed in species of *Atelopus* (Kaplan 1997). Furthermore, the recordings showed minor cyclic activity in the anterior part of the abdominal sucker (region of branchial chambers) while animals rested in attached position. This indicated that the tadpoles ventilated while being attached (see Gradwell 1971, 1973, for general ventilating mechanism, see Gradwell 1968, 1972a,b; Gradwell and Pasztor 1968; Larson and Reilly 2003). We found no radical structural changes in the musculoskeletal architecture that could indicate that the process of ventilation is different in the taxa examined, despite some muscles acquired functions related to abdominal suction.

Some other species that inhabit lotic environments (suctorial tadpoles of *Ascaphus*, *Boophis*, *Heleophryne*, *Hyloscirtus*, *Hypsiboas*, *Litoria* and the fossorial tadpoles of *Leptobrachella mjobergi* Smith, 1925) have well-developed m. rectus abdominis and m. rectus cervicis that extend far anteriorly (level of palatoquadrate or cartilago meckeli). These muscles have been speculated to pull the body close to the substrate and assist in lower jaw abduction (Noble 1929; Gradwell 1973; Haas and Richards 1998; Haas et al. 2006). Such anterior extension of these muscles is absent in *H. cavitympanum* and *M. jerboa* tadpoles; rather, slips of the m. rectus abdominis connect to soft tissue at the posterior base of the abdominal sucker, as has been reported in *Amolops ricketti* (Noble 1929).

Some skeletal features have been reported consistently in studies on lotic tadpoles of distant lineages and, therefore, have been correlated with this particular way of life (Noble 1929; Wassersug and Hoff 1979; McCranie et al. 1989; Lavilla and de la Riva 1993; Haas and Richards 1998; Lavilla and de Sá 2001; Aguilar et al. 2007; Aguayo et al. 2009; present study): Broad, long and partially fused cornua trabeculae; strong, short and wide pars articularis quadrati; relatively small branchial basket and enlarged ceratohyals; and tendency to reduced Ceratobranchial IV have evolved convergently in different lineages that have become suctorial.

Evolution of ranid gastromyzophorous tadpoles

Asian cascade frogs of the genera *Huia* and *Meristogenys* are endemic to Sundaland; the distribution of *Amolops* species covers Nepal, northern India, western and southern China to Malaya (Frost 2015). These frogs live along rocky streams and their tadpoles are gastromyzophorous. The presence of an abdominal sucker goes along with a hydrodynamically optimized body shape. They graze on organic overgrowth on rocks, both inside the water and outside in the spray zone (AH personal observation for several *Meristogenys* species). Species with this tadpole type are highly dependent on the availability of suitable rocky streams as larval habitats. Thus, these morphological and ecological features of tadpoles in the three genera are linked to a specific microhabitat in Sundaland.

In *Rana sauteri* from Taiwan, a rheophilous tadpole with an abdominal sucker has been described (Kuramoto et al. 1984; Chou and Lin 1997). However, the edge of the abdominal sucker in *R. sauteri* is not sharply defined as in *Amolops*, *Huia* and *Meristogenys*, where the rim of the sucker is completely free and raised, especially at the posterior circumference (Kuramoto et al. 1984). Moreover, the m. diaphragmatopraecordialis, which pulls up the floor of the sucker to generate negative pressure, is absent in *R. sauteri* (Kuramoto et al. 1984), but well developed in *Amolops*, *Huia* and *Meristogenys*. The lack of these derived anatomical characters in combination with the less developed adaptations to strong currents in external morphology (narrow oral sucker and large dorsal tail fin) and the distant phylogenetic position (Pyron and Wiens 2011) support the hypothesis that the rheophilous tadpoles in *R. sauteri* evolved independently by convergent adaptation; therefore, we neglect the larvae of *R. sauteri* in further considerations below and in Fig. 8.

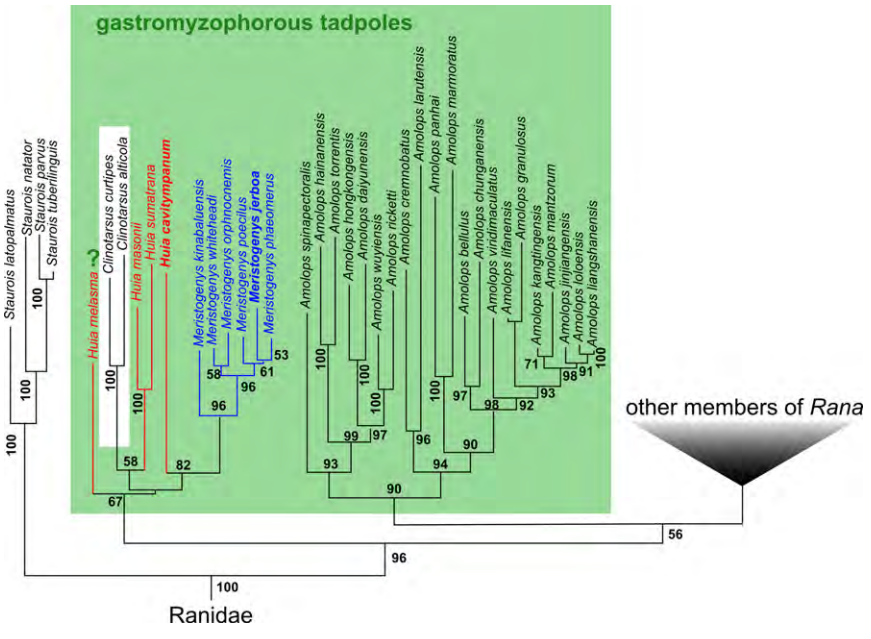

Fig. 8. Current phylogenetic hyopothesis, redrawn with modifications from Pyron and Wiens (2011). Taxa names according to Frost (2015). The tree shows the current phylogenetic position of the taxa discussed herein and their relatives. Although several nodes show high support values, some nodes crucial for the understanding of the evolution of abdominal sucker bearing tadpoles are weakly supported. This particularly questions the position of *Clinotarsus curtipes* and *C. alticola* that both do not possess gastromyzophorous tadpole (Hiragond and Shanbhag 2001; Grosjean et al. 2003). The tadpole of *Huia melasma* has not been described yet, but the ecology of the adults (Stuart and Chan-Ard 2005) let us assume a gastromyzophorous tadpole for the sake of this argumentation.

One may expect that the ecological strategy and large number of congruent anatomical details in the specific Asian gastromyzophorous morphotype evolved only once. This consideration led Inger (1966) to argue that the gastromyzophorous tadpole should define one genus, that is *Amolops*. Later, however, Yang (1991) split up Inger's *Amolops* into *Amolops*, *Meristogenys* and *Huia*, based on larval and adult morphological characters. In his phylogenetic analysis, Yang identified one derived character state in favour of Huia and *Meristogenys*, respectively: Scattered glands present on the back of the tadpoles in *Huia*, while in *Meristogenys* the keratinized portion of the upper beak is divided and its outer surface is ribbed (Inger 1985). Matsui et al. (2006) and Cai et al. (2007) included the type species *H. cavitympanum* in their studies but could not corroborate *Huia* monophyly. The morphological defining characters that Yang (1991) had used and the monophyly of *Huia* were questioned by molecular analyses (Stuart 2008). The genus *Huia* expanded temporarily to include 47 ranid species under the name (Frost et al. 2006), only until others rejected this proposal (Stuart 2008; Pyron and Wiens 2011) and argued for a reduced number of species of *Huia*. These latter two more recent phylogenetic analyses have not confirmed a clade *Huia* + *Meristogenys* + *Amolops* (see Fig. 8). They found *Meristogenys* and *Amolops* to be monophyletic, respectively, but not *Huia*. Within *Huia*, *H. cavitympanum* was retrieved in a clade with *Meristogenys* (forming a strictly Bornean clade), whereas *H. sumatrana* (Sumatra), *H. melasma* (Thailand) and *H. masonii* (Java) grouped in a clade with the Indian *Clinotarsus curtipes* (Jerdon, 1853) and *C. alticola* (Boulenger, 1882); the latter both have non-gastromyzophorous tadpoles (Hiragond and Shanbhag 2001; Grosjean et al. 2003). According to this hypothesis, the gastromyzophorous tadpole type evolved twice (Fig. 8): in the *Meristogenys* + *Huia* clade, and in *Amolops*; it would have been lost in the clade combining *C. alticola* and *C. curtipes* (Pyron and Wiens 2011). The support values for crucial nodes at the base of the *Huia* + *Meristogenys*-clade and the *C. curtipes* + *C. alticola*-clade, respectively, were particularly low in the tree of Pyron and Wiens (2011). The high degree of congruence in the anatomy of the ventral sucker and in the external morphology of the tadpoles of *Amolops*, *Huia* and *Meristogenys* challenges their phylogenetic hypothesis. The morphological evidence, with a large number of shared anatomical details and shared ecology, challenge the view of a convergent origin of this specific gastromyzophorous morphotype in the *Meristogenys, Huia* and *Amolops*. A broader taxon and character sampling is needed to resolve the phylogenetic relationships of the Asian cascade frogs reliably and to shed light on the evolution of the gastromyzophorous tadpole morphotype in ranids.

Acknowledgements

We are grateful to Sarawak Forest Department, in particular Datuk Cheong Ek Choon, Director, and Bolhan Budeng, for issuing collecting permits (NPW.907.4–36) and export permits. The Economic Planning Unit, The Prime Minister's Department, Malaysia, and especially Mrs. Munirah Abd. Manan were supportive in issuing research permit No. 1168 to A. Haas. We are thankful to Sabah Parks, especially Jamili Nais, who supported this project by providing research permit TS/PTD/5/4. We received excellent help from A.M. Vogt who assisted in producing some of the serial sections and cleared and stained specimens. We are deeply indebted to two anonymous reviewers who made valuable suggestions. We gratefully acknowledge funding of the Volkswagen Foundation, Germany (Grant I/79 405 to AH and ID), Naturhistorisches Museum der Burgergemeinde Bern, Universität Hamburg, and Universiti Malaysia Sarawak.

References

Ablan D (2008) Official Luxology Modo 301 Guide. Course Technology, Cengage Learning, Boston.

Aguayo R, Lavilla E, Vera Candioti MF, Camacho T (2009) Living in fast-flowing water: morphology of the gastromyzophorous tadpole of the bufonid *Rhinella quechua* (*R. veraguensis* group). J Morphol **270**:1431–1442.

Aguilar CA, Siu-Ting K, Venegas P (2007) The rheophilous tadpole of *Telmatobius atahualpai* Wiens, 1993 (Anura: Ceratophryidae). South Am J Herpetol **2**:165–174.

Altig R, Johnston GF (1989) Guilds of anuran larvae: relationships among developmental modes, morphologies, and habitats. Herpetol Monogr **3**:81–109.

Altig R, McDiarmid RW (1999) Diversity. Familial and generic characterizations. In: Altig R, McDiarmid RW (eds), Tadpoles. The Biology of Anuran Larvae. University of Chicago Press, Chicago and London, pp 295–337.

Annandale N, Hora SL (1922) Parallel evolution in the fish and tadpoles of mountains torrents. Rec Indian Mus **24**:505–510.

de Beer GR (1937) The Development of the Vertebrate Skull. The Clarendon Press, Oxford.

Boistel R, Grosjean S, Lötters S (2005) Tadpole of *Atelopus franciscus* from French Guyana, with comments on other larvae of the genus (Anura: Bufonidae). J Herpetol **39**:148–153.

Brower AVZ, Schawaroch V (1996) Three steps of homology assessment. Cladistics **12**:265–272.

Cadle JE, Altig R (1991) Two lotic tadpoles from the Andes of southern Peru: *Hyla armata* and *Bufo veraguensis*, with notes on the call of *Hyla armata* (Amphibia, Anura: Hylidae and Bufonidae). Stud Neotrop Fauna Environ **26**:45–53.

Cai H-X, Che J, Pang JF, Zhao EM, Zhang YP (2007) Paraphyly of Chinese *Amolops* (Anura, Ranidae) and phylogenetic position of the rare Chinese frog, *Amolops tormotus*. Zootaxa **1531**:49–55.

Chou W, Lin J (1997) Tadpoles of Taiwan. Natl Mus Nat Sci Spec Pub **7**:1–98.

Coloma LA (2002) Two new species of *Atelopus* (Anura: Bufonidae) from Ecuador. Herpetologica **58**:229–252.

Dietrich HF, Fontaine AR (1975) A decalcification method for ultrastructure of echinoderm tissues. Stain Tech. **50**:351–354.

Dingerkus G, Uhler LD (1977) Enzyme clearing of Alcian Blue stained whole small vertebrates for demonstration of cartilage. Stain Technol **52**(4):229–232.

Duellman WE, Lynch JD (1969) Descriptions of *Atelopus* tadpoles and their relevance on atelopodid classification. Herpetologica **25**:231–240.

Frost DR (2015) Amphibian Species of the World: An Online Reference. Version 6.0. American Museum of Natural History, New York, NY. Electronic Database accessible at http://research.amnh.org/herpetology/amphibia/index.html (accessed 30.08.2015).

Frost DR, Grant T, Faivovich J, Bain RH, Haas A, Haddad CFB, de Sá RO, Channing A, Wilkinson M, Donnellan SC, Raxworthy CJ, Campbell JA, Blotto BL, Moler P, Drewes RC, Nussbaum RA, Lynch JD, Green DM, Wheeler WC (2006) The amphibian tree of life. Bull Am Mus Nat Hist **297**:1–370.

Gascon C (1989) The tadpole of *Atelopus pulcher* Boulenger (Anura, Bufonidae) from Manaus, Amazonas. Rev Bras Zool **6**:235–239.

Gaupp E (1893) Beitraege zur Morphologie des Schaedels. I Primordial-Cranium und Kieferbogen von *Rana fusca*. Morphol Arbeit **2**:275–481.

Gaupp E (1894) Beitraege zur Morphologie des Schaedels. II. Das Hyobranchial-Skelet der Anuren und seine Umwandlung. Morphol Arbeit **3**:389–437.

Gosner KL (1960) A simplified table for staging anuran embryos and larvae with notes on identification. Herpetologica **16**:183–190.

Gradwell N (1968) The jaw and hyoidean mechanism of the bullfrog tadpole during aqueous ventilation. Can J Zool **46**:1041–1052.

Gradwell N (1971) Experiments on the suction and gill irrigation mechanisms. Canad J Zool **49**:307–332.

Gradwell N (1972a) Gill irrigation in *Rana catesbeiana*. Part I. On the anatomical basis. Canad J Zool **50**:481–499.

Gradwell N (1972b) Gill irrigation in *Rana catesbeiana*. Part II. On the musculoskeletal mechanism. Canad J Zool **50**:501–521.

Gradwell N (1973) On the functional morphology of suction and gill irrigation on the tadpole of *Ascaphus*, and notes on hibernation. Herpetologica **29**:84–93.

Gradwell N, Pasztor VM (1968) Hydrostatic pressures during normal ventilation in the bullfrog tadpole. Can J Zool **46**:1169–1174.

Gray P, Cannatella DC (1985) A new species of *Atelopus* (Anura: Bufonidae) from the Andes of northern Peru. Copeia **1985**:910–919.

Grosjean S, Perez M, Ohler A (2003) Morphology and buccopharyngeal anatomy of the tadpole of *Rana* (*Nasirana*) *alticola* (Anura: Ranidae). Raff Bull Zool **51**:101–107.

Haas A (1997) The larval hyobranchial apparatus of discoglossoid frogs: its structure and bearing on the systematics of the Anura (Amphibia: Anura). J Zool Syst Evol Res **35**:179–197.

Haas A (2003) The phylogeny of frogs as inferred from primarily larval characters (Amphibia, Anura). Cladistics **19**:23–89.

Haas A, Richards SJ (1998) Correlations of cranial morphology, ecology, and evolution in Australian suctorial tadpoles of the genera *Litoria* and *Nyctimystes* (Amphibia: Anura: Hylidae: Pelodryadinae). J Morphol **238**:109–141.

Haas A, Hertwig S, Das I (2006) Extreme tadpoles: the morphology of the fossorial megophryid larva, *Leptobrachella mjobergi*. Zoology **109**:26–42.

Haas A, Wolter J, Hertwig ST, Das I (2009) Larval morphologies of three species of stream toads, genus *Ansonia* (Amphibia: Bufonidae) from East Malaysia (Borneo), with a key to known Bornean *Ansonia* tadpoles. Zootaxa **2302**:1–18.

Hiragond NC, Shanbhag BA (2001) Description of the tadpole of a stream breeding frog, *Rana curtipes*. J Herpetol **35**:166–168.

Hora SL (1923) Observations of the fauna of certain torrential streams in the Khasi Hills. Rec Indian Mus **25**:581–599.

Hora SL (1930) Ecology, bionomics and evolution of the torrential fauna with special reference to the organs of attachment. Philos Trans R Soc Lond B Biol Sci **218**:171–282.

Inger RF (1966) The systematics and zoogeography of the Amphibia of Borneo. Fieldiana Zool (NS) **52**:1–402.

Inger RF (1985) Tadpoles of the forested regions of Borneo. Fieldiana Zool (NS) **26**:1–89.

Inger RF (1992) Variation of apomorphic characters in stream-dwelling tadpoles of the bufonid genus *Ansonia* (Amphibia: Anura). Zool J Linn Soc **105**:225–237.

de Jongh HJ (1968) Functional morphology of the jaw apparatus of larval and metamorphosing *Rana temporaria*. Neth J Zool **18**:1–103.

Kaplan M (1997) Internal and external anatomy of the abdominal disc of *Atelopus* (Bufonidae) larvae. Caldasia **19**:61–69.

Kleinteich T, Haas A (2006) Cranial musculature in the larva of the caecilian, *Ichthyophis kohtaoensis* (Lissamphibia: Gymnophiona). J Morphol **268**:74–88.

Kleinteich T, Haas A (2011) The hyal and ventral branchial muscles in caecilian and salamander larvae: homologies and evolution. J Morphol **272**:598–613.

Kuramoto M, Wang C, Yü HT (1984) Breeding, larval morphology and experimental hybridization of the Taiwanese brown frogs, *Rana longicrus* and *R. sauteri*. J Herpetol **18**:387–395.

Larson PM, Reilly SM (2003) Functional morphology of feeding and gill irrigation in the anuran tadpole: electromyography and muscle function in larval *Rana catesbeiana*. J Morphol **255**:202–214.

Lavilla EO (1988) Lower *Telmatobiinae* (Anura: Leptodactylidae): generic diagnoses based on larval characters. Occas Pap Mus Nat Hist Univ Kansas **124**:1–19.

Lavilla EO, de la Riva I (1993) La larva de *Telmatobius bolivianus* (Anura. Leptodactylidae). Alytes **11**:37–46.

Lavilla EO, de Sá RO (2001) Chondrocranium and visceral skeleton of *Atelopus tricolor* and *Atelophryniscus chrysophorus* (Anura: Bufonidae). Amphib-Reptil **22**:167–178.

Lavilla EO, de Sá R, De La Riva I (1997) Description of the tadpole of *Atelopus tricolor* (Anura: Bufonidae). J Herpetol **31**:121–124.

Lescure J (1981) Contribution á l'étude des amphibiens de Guyane Française. IX. Le têtard gastromyzophore d'*Atelopus avescens* Duméril et Bibron (Anura, Bufonidae). Amphib-Reptil **2**:209–215.

Lindquist ED, Hetherington TE (1988) Tadpoles and juveniles of the Panamanian golden frog, *Atelopus zeteki* (Bufonidae), with information on the development of coloration and patterning. Herpetologica **54**:370–376.

Lynch JD (1986) Notes on the development of *Atelopus subornatus*. J Herpetol **20**:126–129.

Malkmus R, Manthey U, Vogel G, Hoffmann P, Kosuch J (2002) Amphibians and Reptiles of Mount Kinabalu (North Borneo). A.R.G. Gantner KG, Koeltz Scientific Books, Koenigstein.
Matsui M (1986) Three new species of *Amolops* from Borneo (Amphibia, Anura, Ranidae). Copeia **1986**:623–630.
Matsui M, Khonsue W, Nabhitabhata J (2005) A new *Ansonia* from the Isthmus of Kra. Thailand (Amphibia, Anura, Bufonidae). Zool Sci **22**:809–814.
Matsui M, Shimada T, Liu WZ, Maryati M, Khonsue W, Orlov N (2006) Phylogenetic relationships of Oriental torrent frogs in the genus *Amolops* and its allies (Amphibia. Anura, Ranidae). Mol Phylogenet Evol **38**:659–666.
Matsui M, Yambun P, Sudin A (2007) Taxonomic relationships of *Ansonia anotis* (Inger, Tan, and Yambun, 2001) and *Pedostibes maculatus* (Mocquard, 1890), with a description of a new genus (Amphibia, Bufonidae). Zool Sci **24**:1159–1166.
McCranie JR, Wilson LD, Williams KL (1989) A new genus and species of toad (Anura: Bufonidae) with an extraordinary stream adapted tadpole from northern Honduras. Occas Pap Mus Nat Hist Univ Kansas **129**:1–18.
McDiarmid RW, Altig R (1999) Tadpoles. The Biology of Anuran Larvae. Altig R, McDiarmid RW (eds). University of Chicago Press, Chicago and London.
Mebs D (1980) Zur Fortpflanzung von *Atelopus cruciger* (Amphibia: Salientia: Bufonidae). Salamandra **16**:65–81.
Mulisch M, Welsch U (2010) Romeis-Mikroskopische Technik. Spektrum Akademischer Verlag, Heidelberg.
Ngo A, Murphy RW, Liu W, Lathrop A, Orlov NL (2006) The phylogenetic relationships of the Chinese and Vietnamese waterfall frogs of the genus *Amolops*. Amphib-Reptil **27**:81–92.
Noble GK (1929) The adaptive modifications of the arboreal tadpoles of *Hoplophryne* and the torrent tadpoles of *Staurois*. Bull Am Mus Nat Hist **58**:291–334.
Nodzenski E, Inger R (1990) Uncoupling of related structural changes in metamorphosing torrent-dwelling tadpoles. Copeia **1990**:1047–1054.
Patterson C (1982) Morphological characters and homology. In: Joysey KA, Friday AE (eds), Problems of Phylogenetic Reconstruction. Academic Press, London, New York, pp 21–74.
de Pinna MCC (1991) Concepts and tests of homology in the cladistic paradigm. Cladistics **7**:367–394.
Pramuk J, Lehr E (2005) Taxonomic status of *Atelophryniscus chrysophorus* (Anura: Bufonidae) inferred from phylogeny. J Herpetol **39**:610–618.
Pyron A, Wiens JJ (2011) A large-scale phylogeny of Amphibia with over 2.800 species, and a revised classification of extant frogs, salamanders, and caecilians. Mol Phylogenet Evol **61**:543–583.
Randrianiaina RD, Strauß A, Glos J, Vences M (2012) Diversity of the strongly rheophilous tadpoles of Malagasy tree frogs, genus *Boophis* (Anura, Mantellidae), and identification of new candidate species via larval DNA sequence and morphology. ZooKeys **178**:59–124.
Rao D, Yang D (1994) The study of early development and evolution of *Torrentophryne aspinia*. Zool Res **15**:142–157.
Richter SS (2005) Homologies in phylogenetic analyses – concept and tests. Theory Biosci **124**:105–120.
Rieppel O, Kearney M (2002) Similarity. Biol J Linn Soc **75**:59–82.
Roček Z (2003) Larval development and evolutionary origin of the anuran skull. In: Heatwole H, Davies M (eds) Amphibian Biology, Vol. 5, Chapter 7. Surrey Beatty, Sons PTY Limited, Chipping Norton, pp 1877–1995.
Rueda-Solano LA, Vargas-Salinas F, Rivera-Correa M (2015) The highland tadpole of the harlequin frog *Atelopus carrikeri* (Anura: Bufonidae) with an analysis of its microhabitat preferences. Salamandra **51**:25–32.
Shimada T, Matsui M, Mohamed M (2007a) Ontogenetic changes in some larval characters of a species tentatively identified to *Meristogenys amoropalamus* (Anura, Ranidae). Curr Herpetol **26**:59–63.
Shimada T, Matsui M, Nishikawa K, Eto K (2015) A New Species of Meristogenys (Anura: Ranidae) from Sarawak, Borneo. ZOO SCI **32**:474–484.
Shimada T, Matsui M, Sudin A, Mohamed M (2007b) Identity of larval *Meristogenys* from a single stream in Sabah, Malaysia (Amphibia: Ranidae). Zool J Linn Soc **151**:173–189.
Shimada T, Matsui M, Yambun P, Sudin A (2011) A taxonomic study of Whitehead's torrent frog, *Meristogenys whiteheadi*, with descriptions of two new species (Amphibia: Ranidae). Zool J Linn Soc **161**:157–183.
Starrett PH (1967) Observations on the life history of the frogs of the family Atelopodidae. Herpetologica **23**:195–204.
Stuart BL (2008) The phylogenetic problem of *Huia* (Amphibia: Ranidae). Mol Phyl Evol **46**:49–60.
Stuart BL, Chan-Ard T (2005) Two new *Huia* (Amphibia: Ranidae) from Laos and Thailand. Copeia **2005**:279–289.
Taylor W, van Dijk GC (1985) Revised procedures for staining and clearing small fishes and other vertebrates for bone and cartilage study. Cybium **9**:107–119.
Vera Candioti MF (2005) Morphology and feeding in tadpoles of *Ceratophrys cranwelli* (Anura: Leptodactylidae). Acta Zool **86**:1–11.
Vera Candioti MF, Lavilla EO, Echeverr, ADD (2004) Feeding mechanisms in two treefrogs, *Hyla nana* and *Scinax nasicus* (Anura: Hylidae). J Morphol **261**:206–224.
Wassersug RJ, Hoff K (1979) A comparative study of the buccal pumping mechanism of tadpoles. Biol J Linn Soc **12**:225–259.
Weninger WJ, Meng S, Streicher J, Müller GB (1998) A new episcopic method for rapid 3-D reconstruction: applications in anatomy and embryology. Anat Embryol **197**:341–348.
Wiens JJ, Sukumaran J, Pyron RA, Brown RM (2009) Evolutionary and biogeographic origins of high tropical diversity in Old World frogs (Ranidae). Evolution **63**:1217–1231.
Yang DT (1991) Phylogenetic systematics of the *Amolops* groups of ranid frogs of southeastern Asia and the Greater Sunda Islands. Fieldiana Zool (NS) **1423**:1–42.
Zachariah A, Abraham RK, Das S, Altig R (2012) A detailed account of the reproductive strategy and developmental stages of *Nasikabatrachus sahyadrensis* (Anura: Nasikabatrachidae), the only extant member of an archaic frog lineage. Zootaxa **3510**:53–64.

Supporting Information

Additional Supporting Information may be found in the online version of this article:

Video S1. Tadpole of *M. jerboa* filmed in the field in a glass aquarium. Video sequences (420 frames per second), recorded with a Casio Exilim EX FH20 camera.